Unusual Trigonal-Planar Copper Configuration Revealed in the Atomic Structure of Yeast Copper−Zinc Superoxide Dismutase[†,‡]

Nancy L. Ogihara,[§] Hans E. Parge,[||,⊥] P. John Hart,[§] Manfred S. Weiss,[§] Joy J. Goto,[#] Brian R. Crane,[||] Joyce Tsang,[||] Kelly Slater,[||] James A. Roe,[▽] Joan Selverstone Valentine,*[,#] David Eisenberg,*[,§] and John A. Tainer*[,||]

UCLA-DOE Laboratory of Structural Biology and Molecular Medicine, Box 951570, University of California, Los Angeles, Los Angeles, California 90095-1570, Department of Molecular Biology, Research Institute of Scripps Clinic, La Jolla, California 92037, Department of Chemistry and Biochemistry, Box 951569, University of California, Los Angeles, Los Angeles, California, 90095-1569, and Department of Chemistry and Biochemistry, Loyola Marymount University, Los Angeles, California 90045

Received August 16, 1995; Revised Manuscript Received November 21, 1995[⊗]

ABSTRACT: The three-dimensional structure of yeast copper−zinc superoxide dismutase (CuZnSOD) has been determined in a new crystal form in space group *R*32 and refined against X-ray diffraction data using difference Fourier and restrained crystallographic refinement techniques. The unexpected result is that the copper ion has moved approximately 1 Å from its position in previously reported CuZnSOD models, the copper−imidazolate bridge is broken, and a roughly trigonal planar ligand geometry characteristic of Cu^{I} rather than Cu^{II} is revealed. Final *R* values for the two nearly identical room temperature structures are 18.6% for all 19 149 reflections in the 10.0−1.7 Å resolution range and 18.2% for 17 682 reflections ($F > 2\sigma$) in the 10.0−1.73 Å resolution range. A third structure has been determined using X-ray data collected at −180 °C. The final *R* value for this structure is 19.0% (R_{free} = 22.9%) for all 24 356 reflections in the 10.0−1.55 Å resolution range. Virtually no change in the positions of the ligands to the zinc center is observed in these models. The origin of the broken bridge and altered Cu−ligand geometry is discussed.

Copper−zinc superoxide dismutase (CuZnSOD) catalyzes the disproportionation of superoxide to give dioxygen and hydrogen peroxide ($2\ O_2^{\bullet-} + 2\ H^+ \rightarrow O_2 + H_2O_2$) (Fridovich, 1989). The widely accepted enzymatic mechanism for CuZnSOD involves alternating reduction of the oxidized Cu^{II} form of the enzyme by superoxide, producing dioxygen (reaction 1) and oxidation of the reduced Cu^{I} form by superoxide, producing hydrogen peroxide (reaction 2) (Rotilio et al., 1971; Rotilio et al., 1972; Klug-Roth et al., 1973; Fielden et al., 1974).

$$O_2^{\bullet-} + Cu^{II}ZnSOD \rightarrow O_2 + Cu^{I}ZnSOD \qquad (1)$$

$$O_2^{\bullet-} + 2H^+ + Cu^{I}ZnSOD \rightarrow H_2O_2 + Cu^{II}ZnSOD \qquad (2)$$

Crystallographic determinations of structures of bovine, spinach, human, yeast, and frog CuZnSODs in the oxidized state have been reported (Tainer et al., 1982, 1983; Kitagawa et al., 1991; Djinovic et al., 1992; Parge et al., 1992; Carugo et al., 1994). In each case, the Cu^{2+} and Zn^{2+} ions were reported to be bridged by an imidazolate ring from a histidyl residue of the protein, and the geometry around the Cu^{2+} ion was described as distorted square planar. In addition, spectroscopic studies of the native proteins and their metal-substituted derivatives supported the conclusion that this imidazolate-bridged configuration was present in solution (Valentine & Pantoliano, 1981; Bertini et al., 1985, 1990; Bannister et al., 1987). With respect to the structure of the reduced state of this enzyme, a considerable body of spectroscopic evidence has led to the conclusion that the imidazolate bridge between the Cu and Zn ions is no longer present (Moss & Fee, 1975; Bailey et al., 1980; Bertini et al., 1985) and that the Cu^{I} center is trigonal planar (Blackburn et al., 1984) (reaction 3).

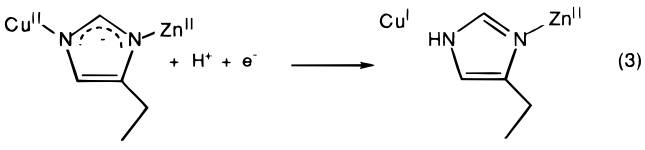

(3)

These conclusions about the presence of the imidazolate bridge in the oxidized and its absence in the reduced enzyme were taken at the time to imply that the bridge must be breaking and reforming during superoxide dismutase catalysis. However, Fee and Bull (1986) reported their determination of the kinetics of this reaction under conditions of saturating superoxide and concluded that, under those conditions, there was not time for the imidazolate bridge to be broken and reformed. They speculated that it is possible for the enzymatic reaction to proceed via a reduced form of the enzyme in which an imidazolate bridge between the Cu^{I}

[†] This research was supported by the National Institutes of Health Chemistry/Biology Interface Predoctoral Training at UCLA (N.L.O.) and in part by an appointment (to P.J.H.) to the Alexander Hollaender Distinguished Postdoctoral Fellowship Program, sponsored by the U. S. Department of Energy, Office of Health and Environmental Research and administered by the Oak Ridge Institute for Science and Education. Work at UCLA was funded by National Institutes of Health Grant GM-28222 (J.S.V.) and Grant GM-31299 (D.E.) and National Science Foundation Grant MCB-9420769 (D.E.). Work at Scripps was funded by National Institutes of Health Grant GM39346 (J.A.T.), and an NSERC graduate fellowship (B.C.).

[‡] The coordinates have been deposited in the Brookhaven Protein Data Bank (file names 1JCW, 1JCV, and 1YSO).

* Authors to whom correspondence should be addressed.

[§] UCLA-DOE Laboratory of Structural Biology and Molecular Medicine.

[||] The Scripps Research Institute.

[⊥] Present address: Agouron Pharmaceuticals, Inc., Department of Crystallography, 3565 General Atomics Court, San Diego, CA 92121.

[#] Department of Chemistry and Biochemistry, UCLA.

[▽] Loyola Marymount University.

[⊗] Abstract published in *Advance ACS Abstracts,* February 1, 1996.

0006-2960/96/0435-2316$12.00/0

and the Zn^{II} centers remained intact (Fee & Bull, 1986). Recently, Banci et al. (1994) reported a crystallographic determination of the reduced form of bovine CuZnSOD in which the imidazolate bridge was found to be intact. By contrast, those same authors demonstrated in an NMR study of reduced human CuZnSOD that the bridge was broken and protonated on the copper side in solution (Banci et al., 1994).

To investigate the state of the copper ion and its ligands in yeast CuZnSOD, we undertook to determine the crystal structure of the wild-type protein. The resultant structure lacks the characteristic imidazolate bridge between the copper and zinc centers found in earlier CuZnSOD structures. In addition, the copper ion is displaced approximately 1 Å from its position in previously reported CuZnSOD structures (Tainer et al., 1982, 1983; Kitagawa et al., 1991; Djinovic et al., 1992; Parge et al., 1992; Carugo et al., 1994) and has only three ligands directly coordinated to it (three His) rather than the five copper ligands observed in earlier structures (four His plus one water).

MATERIALS AND METHODS

Two separate samples, A and B, of CuZnSOD from *Saccharomyces cerevisiae* (YCuZnSOD) from different lots were purchased from Carlbiotech Ltd., Copenhagen.

These two samples were used to obtain room temperature structures A and B in two different labs. Crystals from these samples were grown by the hanging drop vapour diffusion method (McPherson, 1985). The blue lyophilized sample A was dissolved to 15−25 mg mL^{-1} in 50 mM phosphate buffer (pH 7.7) with no further manipulation of the protein, whereas for sample B the enzyme was dialyzed into 50 mM phosphate buffer at pH 7.7. The resulting pale blue protein solution was mixed with an equal volume (generally 5 μL) of reservoir solution containing between 2.0 and 2.3 M ammonium sulfate, 50 mM Tris-HCl, pH 7.5, 50 mM NaCl, and 0.001% (w/v) NaN_3 and allowed to equilibrate at room temperature. Large, colorless, block-like prisms grew within one week in space group $R32$. The hexagonal unit cell parameters were $a = 119.28$ Å and $c = 75.05$ Å. To obtain higher resolution diffraction data with less radiation damage and hence a better quality structure, sample A was also used for cryocrystallographic studies yielding the structure we call A′. Crystals for structure A′ were prepared using a cryoprotectant of 33% glycerol and 67% 2-methyl-2,4-pentanediol and flash-frozen under liquid nitrogen to −180 °C. The unit cell for the frozen form was nearly isomorphous with the room temperature form, with a slight shrinkage of cell parameters to $a = 118.39$ Å, $c = 73.5$ Å leading to a 3.5% reduction in the cell volume.

This combination of space group and unit cell parameters makes the possibility of a dimer in the asymmetric unit unlikely, since the calculated V_m would be outside of the typical range for protein crystals (Matthews, 1968). The calculated V_m with a monomer in the asymmetric unit is 3.2 $Å^3$/Da for structures A and B and 3.1 $Å^3$/Da for structure A′.

Diffraction data were collected independently in two different laboratories (structures A and A′ at UCLA and structure B at Scripps). For structure A and structure A′, data were collected using a Rigaku RAXIS IIc imaging plate detector system. The X-ray source was a Rigaku RU-200 generator with a graphite monochromator operating at 50 kV and 100 mA. The crystal-to-detector distance was 100 mm, and crystals were rotated about the spindle axis with images collected over 1.9° to a resolution of 1.7 Å for structure A and over 1.7° to a resolution of 1.55 Å (2θ setting of 15°) for structure A′. Data were evaluated using the RAXIS processing software (MSC Corp.)

For structure B crystals, diffraction data were measured on a Siemens X-100A multiwire area detector with a three axis camera. X-rays were generated by an Elliot GX-21 rotating anode operated at 40 kV and 50 mA using a 200 μm focus and a nickel filter. Data were collected on one crystal in sweeps of ω using frame widths of 0.25° and 0.10° with 300 and 200 s exposure times per frame, respectively. The crystal-to-detector distance was set to 120 mm and fitted with a helium chamber. Three 2θ settings of 20°, 25°, and 30° were used, corresponding to a maximum resolution of 2.1, 1.9, and 1.7 Å, respectively.

Structure A of YCuZnSOD was solved by molecular replacement using the X-PLOR program package (Brünger, 1988). From the YCuZnSOD structure solved previously in space group $P2_12_12$ at a lower resolution (Djinovic et al., 1992), coordinates of all atoms from the subunit referred to as "monomer A", with the imidazolate bridge intact in the model, were arbitrarily chosen and used as the search model. The orientation and position of the molecule were determined unambiguously by the rotation and translation functions. Rigid body refinement gave an R value of 31.4% for all data between 10.0 and 2.5 Å. Six rounds of refinement at gradually increasing resolution lowered the R factor to 18.6%. We define a round of refinement as sequential utilization of positional, simulated annealing, and restrained isotropic temperature factor refinement routines in X-PLOR or 20 cycles of conjugate gradient minimization in SHELXL93 (Sheldrick & Schneider, 1995) followed by visual inspection of electron density maps with Fourier coefficients of the form $(2F_o - F_c)\alpha_c$ and $(F_o - F_c)\alpha_c$ coupled with manual model building (when necessary) using the graphics program FRODO (Jones, 1982).

For structures A and A′, no stereochemical restraints were imposed on the coordination geometry of active site copper and zinc ions during crystallographic refinement. Simulated annealing omit maps (5000 K) (Hodel et al., 1992) and anomalous difference Fourier omit maps (Strahs & Kraut, 1968) with Cu and Zn removed from the phase calculation were analyzed to verify the Cu and Zn positions.

Structure B was solved by molecular replacement, also using the program package X-PLOR (Brünger, 1988). The A1A2 dimer of human superoxide dismutase (Parge et al., 1992) was used, with amino acid differences incorporated in the model using FRODO (Jones, 1982). Rotation/translation solutions verified that the dimer two-fold axis is coincident with the two-fold axis along a. Rigid body refinement with X-PLOR gave an R factor of 43.2% for all data with $F > 3\sigma$ between 10.0 and 2.5 Å data, which was reduced to 24.2% after further refinement against X-ray data. The model was refit to simulated annealing omit maps calculated for the complete structure at 10-residue intervals with one residue overlap. Further model adjustments and addition of water molecules were performed over an additional rebuilding cycle to 1.73 Å resolution 15-residue sequential omit maps, and three cycles of examining $2F_o - F_c$, and $F_o - F_c$ 1.73 Å resolution maps. Each refitting round was followed by positional and thermal factor refinement

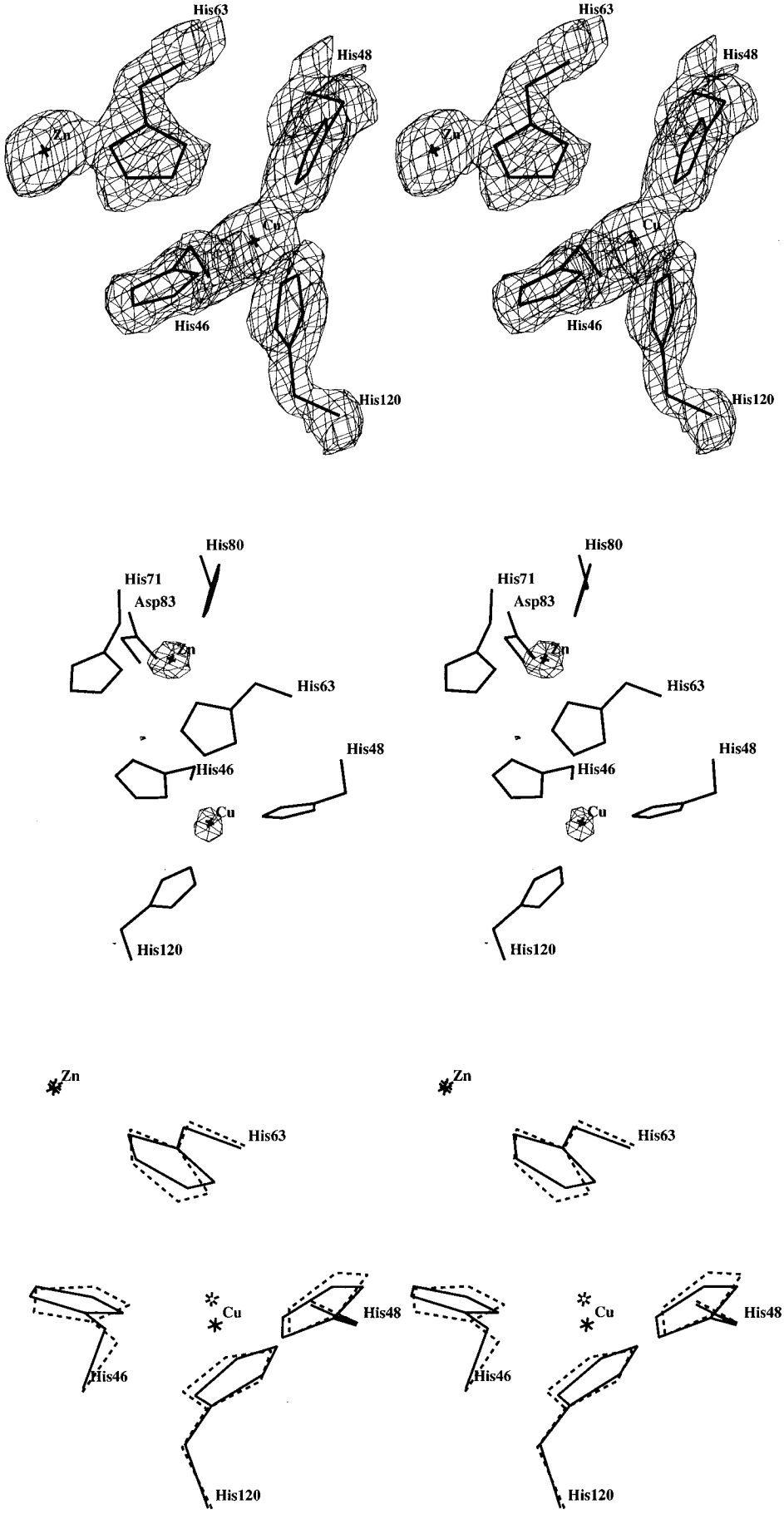
His63
His48
Zn
Cu
His46
His120
His80
His71
Asp83

Table 1: Summary of X-ray Data Collection for Crystals of Yeast Cu−Zn Superoxide Dismutase

yeast Cu/Zn SOD	structure A	structure B	structure A′
unit cell dimensions (Å)	$a = 119.28$, $c = 75.05$	$a = 119.33$, $c = 75.19$	$a = 118.39$, $c = 73.50$
temperature (°C)	20	18	−180
wavelength (Å)	1.54	1.54	1.54
crystal-to-film distance (mm)	100	120	100
oscillation range (deg)	1.9	0.25−0.10[a]	1.70
no. of observations	87 283	102 086	88 085
no. of unique reflections	19 256	20 002	26 394
completeness (%)[b]	82.3 (40.8)[c]	92.4 (40.9)[c]	86.7 (54.6)[c]
resolution limit (Å)	1.70	1.73	1.55
R_{sym} (%)[d]	9.9	6.3	9.2

[a] Data collected in sweeps of ω with frame widths of 0.25° and 0.10°. [b] Of all reflections to the resolution listed. [c] These numbers denote completeness in the highest resolution shells: 1.70−1.76 Å for structure A, 1.73−1.8 Å for structure B, and 1.55−1.61 Å for structure A′. [d] R_{sym} = conventional discrepancy R factor for scaling symmetry-related intensities.

Table 2: Summary of Crystallographic Refinement of Three Models of CuZnSOD, Using the X-PLOR (Brünger, 1988) Program Package[a]

	structure A	structure B	structure A′
temperature (°C)	20	18	−180
no. of rounds	6	7	5
no. of reflections	19 018	17 682	25 275
resolution range (Å)	10.0−1.7	10.0−1.73	10.0−1.55
R (%)	18.6	18.2	19%
R_{free} (%)	*b*	*b*	22.9%
$F/\sigma F$	>0	>2	>0
no. of protein atoms (not hydrogen)	1106	1106	1106
no. of metal ions	2	2	2
no of solvent atoms	108	125	183
rms deviation from ideal values			
bond length (Å)	0.009	0.012	0.010
bond angle (deg)	1.7	2.6	1.9
dihedral angle (deg)	25.3	26.6	24.9
improper angle (deg)	1.3	1.3	1.4

[a] Refined models and the corresponding structure factors have been deposited to the Protein Data Bank. [b] R_{free} not calculated.

with all stereochemical restraints removed from the Cu and Zn coordination geometry. Active site geometry was further assessed by simulated annealed spherical omit maps calculated with all model atoms within a 7 Å radius of each metal ion removed from the phase calculation.

EPR spectra were recorded on a Bruker ER 200D operating at X-band. All spectra were recorded at 111 K, with a microwave power of 20.7 mW, modulation amplitude of 10 G, frequency of 9.55G Hz, time constant of 640 ms, and sweep width of 1600 G with 2046 point resolution. The mother liquor was removed from the single crystal (about 0.5 × 0.5 × 0.25 mm), and spectra were immediately recorded on the sample. The crystal was then redissolved with 10 μL (the original crystallization volume) of 50 mM Tris-HCl, pH 7.5. All handling of the single crystal was done under an atmosphere of argon. After 12 h, spectra were again recorded for the crystal redissolved in the Tris-HCl solution after two exposures to a stream of oxygen for 2−3 min.

RESULTS

Table 1 summarizes the X-ray data collection and processing for the room temperature YCuZnSOD structures A and B and the low temperature structure A′. Refinement statistics for each structure are presented in Table 2.

Structure determination resulted in nearly identical models for YCuZnSOD. In the two room temperature YCuZnSOD structures, A and B, the ligand coordination around the copper center was observed to be trigonal planar, with the copper approximately in the plane of the three ligands and with bond distances and coordination angles as shown in Table 3. In previously determined structures, His63 bridges between the copper and zinc ions, with a Cu···His63−NE2 distance of approximately 2 Å. In the refined structures A, B, and A′, the separations of the Cu···His63−NE2 bond distances were found instead to be 3.16, 2.93, and 3.16 Å, respectively. At these distances of about 3 Å, Cu can no longer be considered bonded to His63−NE2; that is, the imidazolate bridge is broken. In contrast, the Zn position and the conformations of the ligands to the Zn are virtually unchanged from the previously reported yeast CuZnSOD structure (Djinovic et al., 1992).

Crystallographic electron density maps confirm the broken bridge. Figure 1a shows a 1.7 Å simulated annealing omit map with Fourier coefficients $(2F_o - F_c)\alpha_c$ (Hodel et al., 1992) superimposed on the final model of structure A illustrating the Cu···His63 bridge-broken conformation. Figure 1b shows an anomalous scattering difference Fourier map (Strahs & Kraut, 1968), with Cu and Zn ions removed from the phase calculation, superimposed on the final refined model of structure A. This map confirms the positions of the copper and zinc ions by anomalous scattering and is essentially unbiased by the model for the metal centers.

The stereochemistry of the copper center found in our structures A, B, and A' differs from that observed in an earlier yeast CuZnSOD structures (Djinovic et al., 1992). Figure 1c illustrates the difference between the locations of the copper centers and their associated ligands in our yeast CuZnSOD structures and the earlier structure (Djinovic et al., 1992). The Cu···N bond lengths found in structures A, B, and A′ and those found in the previously determined model for YCuZnSOD are given in Table 3.

To investigate the oxidation state of the copper, EPR spectra were recorded of (1) an SOD solution prior to crystallization, (2) a single SOD crystal, (3) the dissolved

FIGURE 1: (a, top) Simulated annealing (5000 K) omit electron density map (Hodel et al., 1992) with Fourier coefficients $(2F_o - F_c)\alpha_c$ for the yeast CuZnSOD active site of structure A contoured at 1σ, shown as a stereopair. This map shows the trigonal planar coordination of Cu by His46, His48, and His120. Notice the broken bridge to His63. Structures B and A' show these same features. (b, middle) Confirmation of the Zn and Cu ion sites in the active site of structure A of yeast CuZnSOD shown by an anomalous Fourier difference map, contoured at 3σ. Notice that the Zn and Cu ions, whose coordinates were determined by refinement against X-ray data, are positioned at the centers of the two peaks of the anomalous difference Fourier map. This map was calculated with coefficients $F(+) - F(-)$ and phases $\alpha - 90°$ (Strahs & Kraut, 1968). (c, bottom) Superposition of structure A (solid lines) with the structure reported by Djinovic et al. (1992) (dashed lines). The positions of the Cu ions differ by 0.59 Å, and the Cu···His63−NE2 distance increases by approximately 1 Å relative to the structure of Djinovic et al. Notice also that His63 of structure A is tilted with respect to the other structure, so that, in combination with the Cu motion, the Cu···NE2 bond is broken (see also panel a).

Table 3: Stereochemical Geometry of the Cu Ion in the Three Models for CuZnSOD Reported Here[a]

	structure A	structure B	structure A′	2.5 Å YCuZnSOD mean (range)[b] (Djinovic et al., 1992)
Cu···His46−ND1	2.06	1.98	2.11	1.86 (1.82−1.91)
Cu···His48−NE2	2.06	2.19	2.07	2.22 (2.13−2.30)
Cu···His63−NE2	3.16	2.93	3.16	2.17 (2.00−2.44)
Cu···His120−NE2	2.10	2.09	2.11	2.16 (2.01−2.26)
Cu···H_2O−O	*c*	3.15[c,d]	*c*	2.03 (1.83−2.37)
His46ND1···Cu···His63−NE2	*e*	*e*	*e*	79.5 (76.2−84.1)
His63−NE2···Cu···His48−NE2	*e*	*e*	*e*	94.2 (90.0−97.9)
His48−NE2···Cu···His120−NE2	118.5	121.8	118.5	105.9 (101.3−109.6)
His120−NE2···Cu···His46−ND1	102.9	99.7	102.3	93.5 (88.8−98.7)
His46−ND1···Cu···His48−NE2	138.5	132.8	139.1	142.7 (139.5−148.2)

[a] In the last column these models are compared to a previously reported X-ray derived model. The copper-to-ligand bond distances are given in angstrøms and the angles in degrees. Amino acid numbers refer to the yeast sequence. [b] According to Djinovic et al. (1992), Cu−ligand bond distances were restrained during crystallographic refinement. We report bond distances and angles averaged over the four molecules in their asymmetric unit. Notice that for one of the four molecules, the Cu···His63−NE2 distance is 2.44 Å despite being restrained to an ideal value of 2.0 Å. [c] Water is not a ligand for these structures. [d] Water could represent a ligand for a five-coordinate minority conformation. [e] The Cu−His63 bridge is broken in these structures.

crystal, and (4) the dissolved crystal exposed to oxygen. As shown in Figure 2, spectra characteristic of Cu^{II} are displayed by the original SOD solution and by the dissolved crystal exposed to O_2. In contrast, the spectra of the crystal and of the dissolved crystal unexposed to O_2, when compared to the oxidized, dissolved crystal, are consistent with Cu^{I} in the crystal.

DISCUSSION

Models A, B, and A′ are very similar. His46, His48, His63, and His120 are in essentially the same positions in the three structures as are the zinc center and its associated ligands, His71, His80, and Asp83. Small differences do exist between structures A and B. When superimposed, the two models differ by 0.12 Å (root-mean-squared deviation of all atoms), about at the level of significance. The most pronounced difference is a 0.2 Å decrease of the Cu···His63−NE2 distance in structure B, toward the five-coordinate conformation. This decrease arises from the combination of a small Cu displacement and a tilt of the His63 imidazole ring. These slight differences may be due to a larger contribution from a minority bridge-bonded five-coordinate Cu species in the B crystals. In support of this, structure B also exhibits a slightly more pronounced elongation of the electron density around the Cu, a slightly smaller distance between the Cu···His63−NE2 than seen in structure A, and a weak water ligand peak at about 3.2 Å from the refined Cu position. Although this minority conformation might be present in all three crystals to a different extent, the major conformation in all three structures has three-coordinate Cu, with no bond bridging to His63.

There are three striking differences between A, B, and A′ and a yeast CuZnSOD structure that was previously determined by Djinovic et al. (1992): (1) the position of the copper ion has shifted by approximately 1 Å relative to His63−NE2 resulting in an increase in the Cu···His63 distance from 2.2 Å (average distance in Djinovic et al. model) to 3.16 (structures A and A′) and 2.93 Å (structure B) in our models; (2) His120 follows this movement of copper while maintaining its coordination bond distance; (3) the Cu is three-coordinate instead of five-coordinate, having an approximately trigonal planar geometry; that is, the Cu forms covalent bonds with His46, His48, and His120, but not His63 or a water ligand. To verify that the geometry around the copper center was not an artifact of partial metal occupancy in the crystal, the occupancies of the Cu and Zn ions were refined against the X-ray data. The resulting peak heights for the copper and zinc atoms refined to the same value (1.04 and 1.02, respectively), consistent with equal occupancy of both metal sites.

The difference between Cu geometry in our structures A, B, and A′ solved in space group *R*32 and the structure solved in space group $P2_12_12$ reported by Djinovic et al. (1992) is large, but its significance is unclear. Possible explanations for the observed differences are the following: (1) specimen handling, (2) different crystallization conditions (ammonium sulfate vs poly(ethylene glycol) (average MW 4000) as precipitant), (3) differences in crystal packing (space group *R*32 vs $P2_12_12$), and (4) different refinement protocols (see Materials and Methods and Table 3).

The copper coordination geometry we observe in A, B, and A′ has not been reported in other CuZnSOD structures. It is three-coordinate, roughly trigonal planar copper coordination geometry, with copper approximately in the plane of the three ligands, and the absence of an imidazolate bridge (see Figure 1a). The first reported crystal structure of a CuZnSOD was of the bovine enzyme (Tainer et al., 1982). It exhibited a five-coordinate copper coordination geometry, with three histidyl imidazoles, a histidyl imidazolate bridging to zinc, and a water molecule as copper ligands. Subsequently determined structures of CuZnSODs gave Cu environments very similar to those reported for the bovine enzyme (Kitagawa et al., 1991; Djinovic et al., 1992; Parge et al., 1992; Carugo et al., 1994).

The copper coordination geometry in A, B, and A′ is one that is much closer to that expected for reduced Cu^{I}-containing, CuZnSOD (Tainer et al., 1983; Roberts et al., 1991; Banci et al., 1994). Thus our model is consistent with reduction of yeast CuZnSOD having occurred under our crystallization conditions. This conclusion is supported by our observation that although the CuZnSOD solution was pale blue and our crystals were colorless. Crystals of Cu^{II}-ZnSOD are typically pale blue. In addition, the EPR spectrum of a crystal showed only a weak Cu^{II} signal, consistent with the majority of the crystals being in the reduced Cu^{I} state, whereas the same crystal dissolved in buffer showed an appearance of the Cu^{II} signal upon exposure to oxygen. Yeast CuZnSOD has been found to be similar

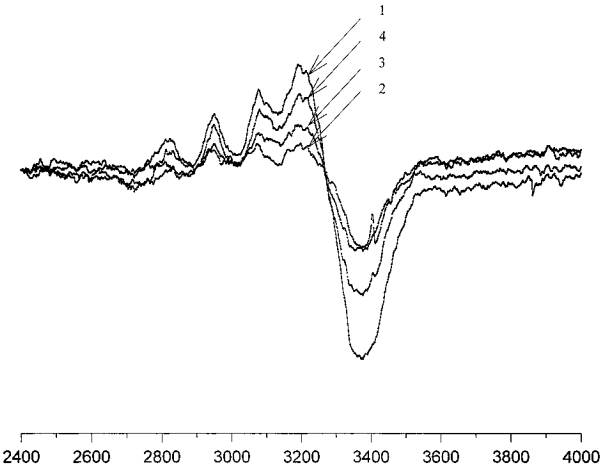

FIGURE 2: EPR spectra (shown in units of Gauss) of yeast SOD in four states: (1) Lyophilized powder dissolved in crystallizing buffer (50 mM Tris-HCl, pH 7.5, with 2.1 M $(NH_4)_2SO_4$ and 50 mM NaCl) to 20 mg/mL; (2) rhombohedral crystal after the mother liquor was removed from around the crystal; (3) crystal dissolved in 50 mM Tris-HCl, pH 7.5, to the same volume as in (1); (4) dissolved crystal 12 h after two 2−3 min exposures to oxygen.

in its reactivity and spectroscopic properties to other characterized CuZnSODs (Valentine & Pantoliano, 1981; Bannister et al., 1987; Bertini et al., 1990), and all of the oxidized CuZnSODs studied thus far have been reported to be stable in solution and in air at room temperature. However, spontaneous reduction of both yeast and bovine CuZnSOD has been observed to occur upon heating (Simonyan & Nalbandyan, 1975; Roe et al., 1988). We speculate that our crystallization conditions may similarly induce reduction of the Cu^{II} to Cu^{I} in CuZnSOD, or select reduced protein from the solution.

Thus, when taken together, the four available yeast CuZnSOD structures suggest that a delicate balance may exist between the reduced and oxidized forms of the enzyme under physiological conditions. As both reduced and oxidized CuZnSOD can react with substrate, an enzyme that is poised to interconvert between reduction states may reflect the attainment of a low activation barrier for the dismutation reaction. The possible influence of crystal lattice contacts on this equilibrium emphasizes the ability of subtle alterations in protein interactions to modulate bound metal ion redox potentials.

CONCLUSIONS

We have determined the three-dimensional crystal structure of yeast copper-zinc superoxide dismutase in a new crystal form, in space group *R*32. Our structure is similar to previously determined models of CuZnSODs, except for a new roughly trigonal-planar coordination geometry around the copper ion and the absence of the imidazolate bridge between the Cu and Zn. From the unexpected Cu coordination geometry, it appears that the enzyme is in a reduced Cu^{I} form as suggested by our EPR experiments. This crystal structure is the first to show a reduced bridge-broken form of CuZnSOD.

REFERENCES

Bailey, D. B., Ellis, P. D., & Fee, J. A. (1980) *Biochemistry 19*, 591−596.

Banci, L., Bertini, I., Bruni, B., Carloni, P., Luchinat, C., Mangani, S., Orioli, P. L., Piccioli, M., Ripneiwski, W., & Wilson, K. (1994) *Biochem. Biophys. Res. Commun. 202*, 1088−1095.

Bannister, J. V., Bannister, W. H., & Rotilio, G. (1987) *CRC Crit. Rev. Biochem. 22*, 111−180.

Bertini, I., Luchinat, C., & Monnanni, R. (1985) *J. Am. Chem. Soc. 107*, 2178−2179.

Bertini, I., Banci, L., Piccioli, M., & Luchinat, C. (1990) *Coord. Chem. Rev. 100*, 67−103.

Blackburn, N. J., Hasnain, S. S., Binsted, N., Diakun, G. P., Garner, C. D., & Knowles, P. F. (1984) *Biochem. J. 219*, 985−990.

Brünger, A. T. (1988) in *Crystallographic Computing 4: Techniques and New Technologies* (Isaacs, N. W., & Taylor, M. R., Eds.) pp 126−140, Clarendon Press, Oxford.

Carugo, K. D., Battistoni, A., Carri, M. T., Polticelli, F., Desideri, A., Rotilio, G., Coda, A., & Bolognesi, M. (1994) *FEBS Lett. 349*, 93−98.

Djinovic, K., Gatti, G., Coda, A., Antolini, L., Pelosi, G., Desideri, A., Falconi, M., Marmocchi, F., Rotilio, G., & Bolognesi, M. (1992) *J. Mol. Biol. 225*, 791−809.

Fee, J. A., & Bull, C. (1986) *J. Biol. Chem. 261*, 13000−13005.

Fielden, E. M., Roberts, P. B., Bray, R. C., Lowe, D. J., Mautner, G. N., Rotilio, G., & Calabrese, L. (1974) *Biochem. J. 139*, 49−60.

Fridovich, I. (1989) *J. Biol. Chem. 264*, 7761−7764.

Hodel, A., Kim, S., & Brunger, A. T. (1992) *Acta Crystallogr. A48*, 851−858.

Jones, T. A. (1982) in *Computational Crystallography* (Sayre, D., Ed.) pp 303−317, Oxford University Press, Oxford.

Kitagawa, Y., Tanaka, N., Hata, Y., Kusunoki, M., Lee, G., Katsube, Y., Asada, K., Aibara, S., & Morita, Y. (1991) *J. Biochem. (Tokyo) 109*, 447−485.

Klug-Roth, D., Fridovich, I., & Rabani, J. (1973) *J. Am. Chem. Soc. 95*, 2786−2790.

Matthews, B. W. (1968) *J. Mol. Biol. 33*, 491−497.

McPherson, A. (1985) *Methods Enzymol. 114*, 120−125.

Moss, T. H., & Fee, J. A. (1975) *Biochem. Biophys. Res. Commun. 66*, 799−808.

Parge, H. E., Hallewell, R. A., & Tainer, J. A. (1992) *Proc. Natl. Acad. Sci. U.S.A. 89*, 6109−6113.

Roberts, V. A., Fisher, C. L., Redford, S. M., McRee, D. E., Parge, H. E., Getzoff, E. D., & Tainer, J. A. (1991) *Free Radical Res. Commun. 12−13*, 269−278.

Roe, J. A., Butler, A., Scholler, D. M., Valentine, J. S., Marky, L., & Breslauer, K. (1988) *Biochemistry 27*, 950−958.

Rotilio, G., Morpurgo, L., Giovagnoli, C., Calabrese, L., & Mondovi, B. (1971) *Biochemistry 11*, 2187−2192.

Rotilio, G., Bray, R. C., & Fielden, E. M. (1972) *Biochim. Biophys. Acta. 268*, 605−609.

Sheldrick, G. M., & Schneider, T. R. (1995) *Methods Enzymol.* (in press).

Simonyan, M. A., & Nalbandyan, R. M. (1975) *Biokhimiya (Moscow) 40*, 727−732.

Strahs, G., & Kraut, J. (1968) *J. Mol. Biol. 35*, 503−512.

Tainer, J. A., Getzoff, E. D., Beem, K. M., Richardson, J. S., & Richardson, D. C. (1982) *J. Mol. Biol. 160*, 181−217.

Tainer, J. A., Getzoff, E. D., Richardson, J. S., & Richardson, D.C. (1983) *Nature 306*, 284−287.

Valentine, J. S., & Pantoliano, M. W. (1981) in *Copper Proteins* (Spiro, T. G., Ed.) pp 292−358, John Wiley and Sons, Inc., New York.

BI951930B